Molecular Therapy
Original Article

PD-L1^{P146R} is prognostic and a negative predictor of response to immunotherapy in gastric cancer

Qing Li,[1,2,9] Zhi-Wei Zhou,[3,9] Jia Lu,[3] Hao Luo,[1,7] Shu-Nan Wang,[4] Yu Peng,[5] Meng-Sheng Deng,[6] Guan-Bin Song,[7] Jian-Min Wang,[6] Xi Wei,[8] Dong Wang,[1] Kenneth D. Westover,[3] and Cheng-Xiong Xu[1,2]

[1]Cancer Center, Daping Hospital, Army Medical University, Chongqing 400042, China; [2]School of Medicine, Chongqing University, Chongqing 400030, China; [3]Department of Radiation Oncology and Biochemistry, University of Texas Southwestern Medical Center, Dallas, TX 75390, USA; [4]Department of Radiology, Daping Hospital, Army Medical University, Chongqing 400042, China; [5]Shanghai Key Laboratory of Regulatory Biology, The Institute of Biomedical Sciences and School of Life Sciences, East China Normal University, Shanghai 200241, China; [6]State Key Laboratory of Trauma, Burn and Combined Injury, Daping Hospital, Army Medical University, Chongqing 400042, China; [7]Key Laboratory of Biorheological Science and Technology, Ministry of Education, College of Bioengineering, Chongqing University, Chongqing 400030, China; [8]Department of Diagnostic Ultrasound, Tianjin Medical University Cancer Institute and Hospital, Tianjin 330006, China

Cancer cells evade immune detection via programmed cell death 1/programmed cell death-ligand 1 (PD-1/PD-L1) interactions that inactivate T cells. PD-1/PD-L1 blockade has become an important therapy in the anti-cancer armamentarium. However, some patients do not benefit from PD-1/PD-L1 blockade despite expressing PD-L1. Here, we screened 101 gastric cancer (GC) patients at diagnosis and 141 healthy control subjects and reported one such subpopulation of GC patients with rs17718883 polymorphism in PD-L1, resulting in a nonsense P146R mutation. We detected rs17718883 in 44% of healthy control subjects, and rs17718883 was associated with a low susceptibility to GC and better prognosis in GC patients. Structural analysis suggests that the mutation weakens the PD-1:PD-L1 interaction. This was supported by co-culture experiments of T cells, with GC cells showing that the P146R substitution results in interferon (IFN)-γ secretion by T cells and enables T cells to suppress GC cell growth. Similar results with animal gastric tumor models were obtained *in vivo*. PD-1 monoclonal antibody treatment did not enhance the inhibitory effect of T cells on GC cells expressing PD-L1^{P146R} *in vitro* or *in vivo*. This study suggests that rs17718883 is common and may be used as a biomarker for exclusion from PD-1/PD-L1 blockade therapy.

INTRODUCTION

Gastric cancer (GC) is the fifth most common malignant tumor and the third leading cause of cancer-related death worldwide.[1] Fewer than 30% of GC patients survive more than 5 years.[2] A contributing factor to the high mortality rate is that more than 70% of patients with GC have advanced-stage disease at diagnosis.[3] First-line treatments are generally toxic, consisting of two-drug cytotoxic regimens such as platinum and fluoropyrimidine, with the addition of trastuzumab for tumors expressing human epidermal growth factor 2.[4] However, recently immunotherapy with pembrolizumab was added as a treatment option based on favorable responses in the KEYNOTE-059 trial.[5]

The human immune system is capable of detecting and eliminating some proportion of tumorigenic cells. However, a subset of cells escape immune detection via activation of an immune checkpoint, leading to tumor growth. This is often accomplished through the programed death protein-1/programed death-ligand 1 (PD-1/PD-L1) axis.[6] PD-L1 is a transmembrane protein that interacts with the PD-1 that is transiently expressed on the surface of activated T cells.[7] Tumor cells inactivate T cells by transmitting negative regulatory signals to T cells via a PD-1:PD-L1 interaction to escape from T cell attack. This allows tumor initiation and progression.[6,8,9] Blockade of the PD-1 and PD-L1 interaction with antibodies restores antitumor immunity.[7] Approximately 40%–57% of GC cases express PD-L1, and PD-L1 expression correlates with tumor size, invasion, and patient survival.[10] This motivated clinical trials of PD-1/PD-L1 blockade for GC. The landmark KEYNOTE-059 trial showed an objective response rate of ∼13% for tumors expressing PD-L1, paving the way for FDA approval of pembrolizumab as a treatment for GC. Although this was an important development for GC treatment, 85% of PD-L1-positive tumors did not respond,[5,11] showing that PD-L1 expression alone is not sufficient to predict patients who will benefit

Received 11 June 2021; accepted 14 September 2021;
https://doi.org/10.1016/j.ymthe.2021.09.013.

[9]These authors contributed equally

Correspondence: Dong Wang, Cancer Center, Daping Hospital, Army Medical University, Chongqing 400042, China.
E-mail: dongwang64@hotmail.com
Correspondence: Kenneth D. Westover, Department of Radiation Oncology and Biochemistry, University of Texas Southwestern Medical Center, Dallas, TX 75390, USA.
E-mail: Kenneth.westover@utsouthwestern.edu
Correspondence: Cheng-Xiong Xu, School of Medicine, Chongqing University, Chongqing 400030, China.
E-mail: xuchengxiong@cqu.edu.cn

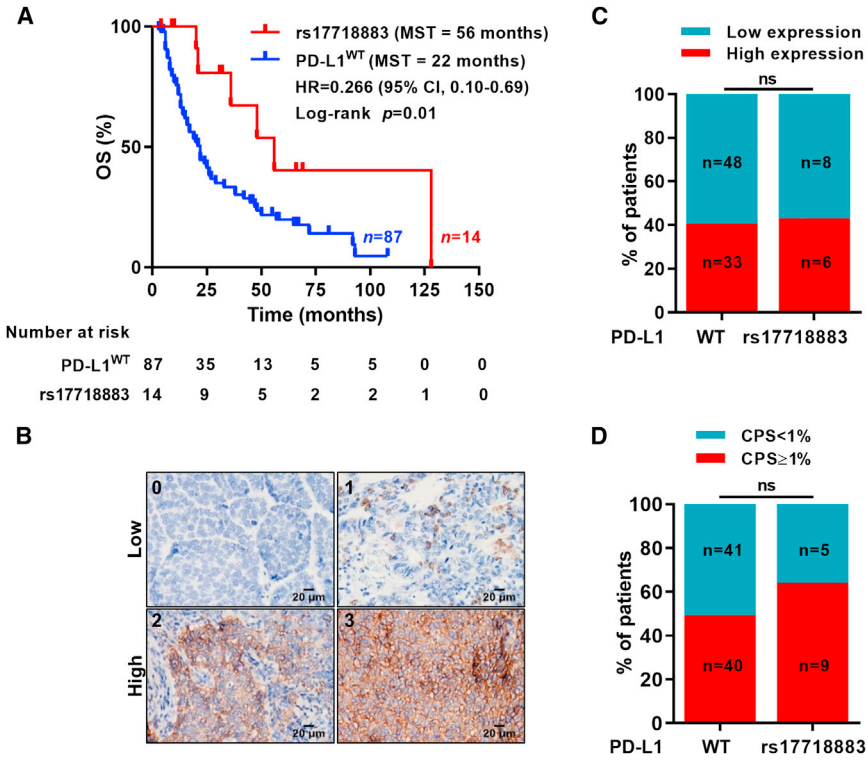

Figure 1. rs17718883 is associated with better overall survival in GC patients

(A) GC patients with rs17718883 have higher overall survival (OS) rate and longer median survival time (MST) relative to counterparts with wild-type (WT) PD-L1. Kaplan-Meier survival curve showing that the PD-L1 rs17718883 polymorphism correlates with OS in patients with GC. rs17718883 was detected in blood samples of 101 GC patients. (B) IHC analysis of PD-L1 expression in GC tissues. Representative images for PD-L1 expression. Magnification, 10×; scale bar, 20 μm. (C and D) The protein expression profile is similar for PD-L1 WT and rs17718883. Correlation between PD-L1 expression level and rs17718883; correlation between rs17718883 and PD-L1 combined positive score (CPS). HR, hazard ratio; CI, confidence interval; ns, no significance.

from PD-1/PD-L1-targeted therapy. The mechanisms of PD-1/PD-L1 resistance in this cancer subtype are not defined.

Single-nucleotide polymorphisms (SNPs) are the most common type of genetic variation, and SNPs are associated with disease development and progression.[12] Several SNPs in the PD-L1 gene have been identified, and some are closely associated with cancer susceptibility, prognosis,[13] and therapeutic efficacy of agents such as chemotherapy[14] and PD-1/PD-L1 blockade.[15] This suggests that PD-L1 SNPs have potential as biomarkers for predicting cancer prognosis and the efficacy of PD-1/PD-L1 blockade therapy. The rs17718883 polymorphism is a common PD-L1 SNP that results in a proline to arginine substitution at residue 146 of PD-L1. This SNP is found in ~17%–46% of healthy individuals.[16,17] rs17718883 is associated with a low susceptibility to liver cancer and a better prognosis in liver cancer patients.[16] These observations suggest that rs17718883 produces a negative effect on PD-L1 function, leading to a change in the natural history of disease processes where PD-L1 is involved. The role of rs17718883 in GC, particularly its impact on the efficacy of immunotherapy, has not been reported.

Here we evaluate the prognostic significance of rs17718883 on GC outcomes. We also provide a structural analysis of PD-L1^{P146R} and explore its impact on the protein dynamics of PD-L1. We also evaluate the impact of PD-L1^{P146R} on immune system function and the efficacy of PD-1/PD-L1 blockade therapy. These results have implications for patient selection for PD-1/PD-L1 blockade therapy.

RESULTS

rs17718883 is associated with low rates of GC and a reduction in GC death

We investigated whether rs17718883 polymorphisms influence clinical outcomes in Chinese GC patients treated in the Cancer Center, Daping Hospital. We compared a population of 141 healthy subjects, age 33–83 years, with 101 GC patients, age 32–87 years, for associations between rs17718883 variations and death. There were more male than female participants in both arms, but the ratios were similar in both groups (Table S1). Genotyping revealed a significant difference in the frequency of rs17718883 variations between patients with GC and healthy control subjects (Table S2 and Figures S1A and S1B). We observed 12.9% (n = 13, $p < 0.001$) of patients with the GC variant and one patient with GG ($p < 0.001$). In contrast, CG was found in 34.0% (n = 48, $p < 0.001$) and GG in 11.4% (n = 16, $p < 0.001$) of healthy control subjects (Table S2). Individuals with the rs17718883 genotype (G/G) or heterozygous genotype (C/G) (both corresponding to a P146R mutation in PD-L1) showed an inverse association with GC compared to patients carrying CC (Table S2). Consistently, a reduced risk of GC was found in individuals carrying the rs17718883 G-allele (n = 15, 7.4%) compared to the C-allele (n = 187, 92.6%) (Table S2). We also found that GC patients carrying the G-allele (C/G+G/G) had a lower rate of lymph node metastasis at 28.6% (n = 14) versus 71.3% (n = 87) (Table S3), longer median survival time (MST = 56 months), and higher overall survival (OS) rate compared to patients with wild-type (WT) PD-L1 (MST = 22 months) ($p = 0.01$) (Figure 1A). Notably, multivariable analyses showed that the rs17718883 G-allele (C/G+G/G) (PD-L1^{P146R}) was an independent predictor of GC patient survival (Table S4). This suggests that the rs17718883 G-allele (hereafter referred to as rs17718883 or PD-L1^{P146R}) plays a suppressive role in GC.

rs17718883 does not affect PD-L1 expression or GC cell growth

One possibility is that cancer-specific survival is better in the context of rs17718883 because it alters expression of PD-L1. Indeed, other PD-L1 polymorphisms have been shown to change PD-L1 expression

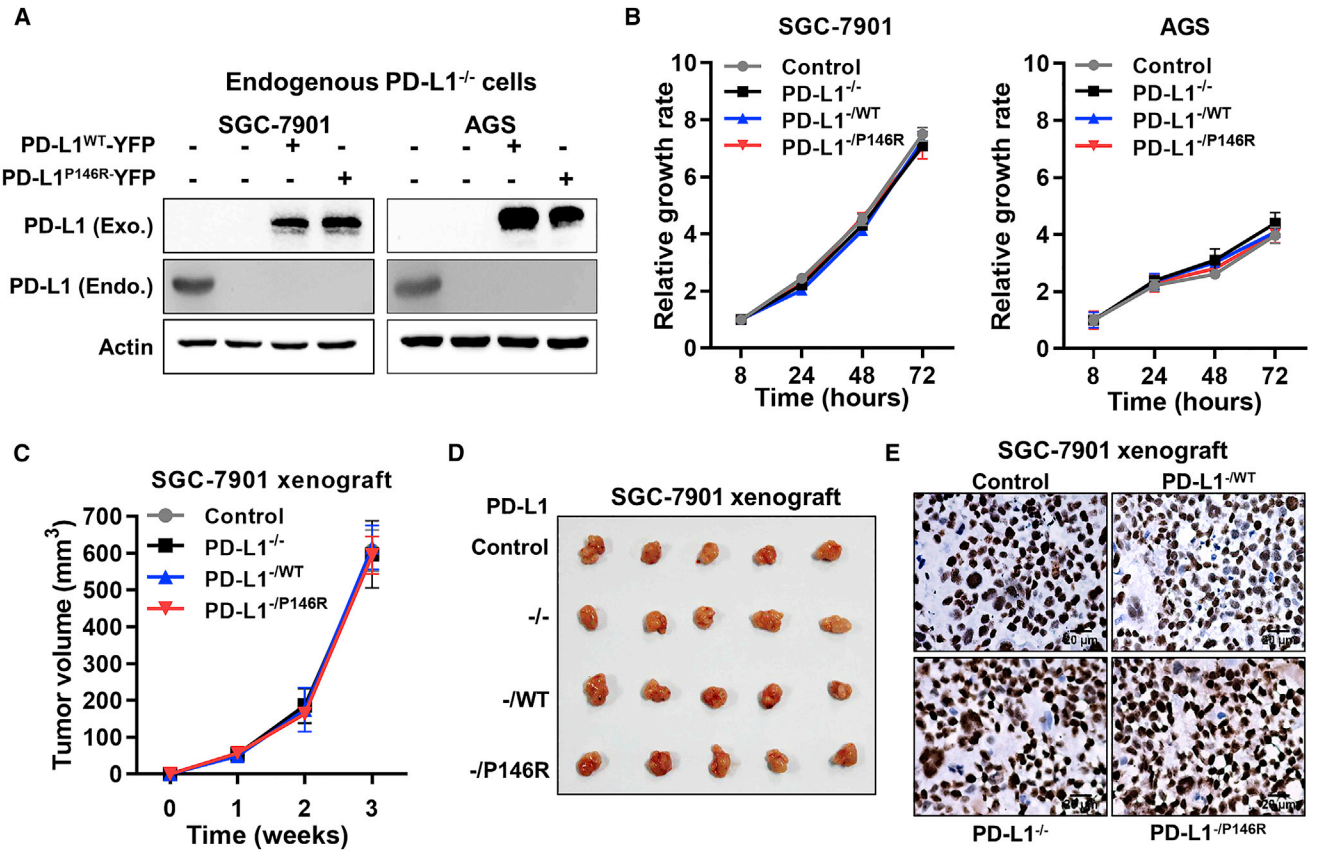

Figure 2. PD-L1^{P146R} does not alter GC growth in the absence of T cells

(A) PD-L1 expression in engineered GC cell lines. Endogenous PD-L1 was knocked out with CRISPR-Cas9 in SGC-7901 and AGS lines (lane 2) and then stably reengineered to express YFP-tagged PD-L1 wild-type (WT) or P146R mutant (lanes 3, 4). (B) PD-L1^{P146R} does not affect the growth rate of engineered SGC-7901 and AGS cells. PD-L1 knockout (PD-L1$^{-/-}$) and overexpression of exogenous WT PD-L1 (PD-L1$^{-/WT}$) or P146R mutated PD-L1 (PD-L1$^{-/P146R}$) did not affect GC cell growth *in vitro*. (C) PD-L1^{P146R} does not affect tumor growth of engineered SGC-7901 xenografts. PD-L1$^{-/-}$ and overexpression of PD-L1$^{-/WT}$ or PD-L1$^{-/P146R}$ did not affect GC growth *in vivo*. (D) Representative images of tumors for engineered SGC-7901 xenografts. (E) PD-L1^{P146R} does not influence cell proliferation in tumors. The expression of Ki-67 in xenograft tumor tissues was detected by IHC. Error bars represent mean ± SD. Magnification, 20×; scale bar, 20 μm. exo, Exogenous; endo, endogenous.

at transcriptional and translational levels.[18] Therefore, we examined the effect of rs17718883 on PD-L1 expression. Immunohistochemistry (IHC) analyses of clinical samples showed no difference in PD-L1 expression between GC with P146R and WT PD-L1 (Figures 1B and 1C). GC patients with positive PD-L1 expression and a combined positive score (CPS) ≥ 1% receive PD-1/PD-L1 blockade therapy.[11] Therefore, we also evaluated for a correlation between P146R and WT PD-L1 for CPS but found none (Figure 1D). Based on these findings we concluded that rs17718883 does not alter the clinical course of GC by changing PD-L1 expression patterns but instead works in concert with PD-1, found on T cells, to exert its effects. We therefore investigated whether PD-L1^{P146R} can function in GC models lacking T cells.

In vitro experiments using the GC cell lines SGC-7901 and AGS showed that the CRISPR-mediated knockout (KO) of endogenous PD-L1 and overexpression of exogenous PD-L1 WT or P146R all gave equivalent growth rates (Figures 2A and 2B). Consistently, xenografts of SGC-7901 cells in nude mice also showed no difference between PD-L1 WT and P146R-expressing lines for tumor growth and body weight (Figures 2C and 2D; Figure S2) or cancer cell proliferation indicated by expression of Ki-67 via IHC (Figure 2E). This confirms that P146R alone does not alter GC progression, suggesting that additional components are required, presumably T cells because PD-L1 plays its crucial role in tumor cells via T cell suppression.

PD-L1^{P146R} impairs PD-L1:PD-L1 and PD-1:PD-L1 interactions in molecular dynamics simulations

rs17718883 results in a missense mutation of proline to arginine at amino acid residue 146 in PD-L1 (Figure 3A). PD-1/PD-L1-mediated tumor immune escape is based on interactions between PD-1 and PD-L1. Based on the location of residue 146 in PD-L1, we hypothesized that a P146R substitution could alter the protein dynamics of PD-L1, leading to changes in PD-L1/PD-L1 and PD-1/PD-L1 complex formation. To assess the protein dynamics of PD-

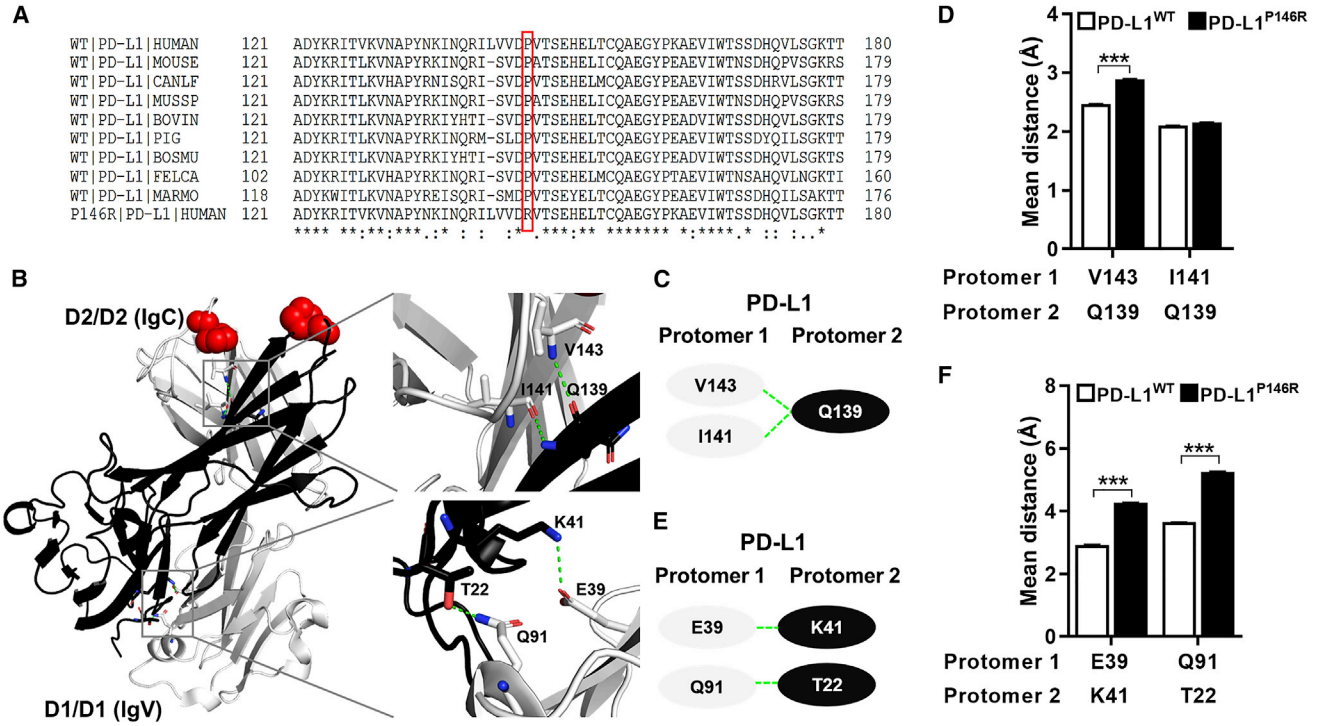

Figure 3. PD-L1^{P146R} alters PD-L1:PD-L1 interactions *in silico*

(A) P146 is conserved across species. (B) Molecular dynamic simulation shows interactions in PD-L1:PD-L1 dimer interface (PDB ID: 3FN3). Residues involved in the hydrogen bonds at the D1/D1 (IgV) and D2/D2 (IgC) dimer interfaces are highlighted as sticks. Proline at 146 is shown in red spheres. Hydrogen bonds involved in the interface are indicated by green dotted line. (C) Schematic of residue contacts at the D2/D2 (IgC) dimer interface. (D) P146R shortens the distance between two PD-L1 protomers at D2/D2 (IgC) dimer interface. Mean distance of residue contacts involved in the D2/D2 (IgC) dimer interface over the MD simulation shows greater distance for P146R. (E) Schematic of residue contacts at the D1/D1 (IgV) dimer interface. (F) P146R widens the distance between two PD-L1 protomers at D1/D1 (IgV) dimer interface. Mean distance of residue contacts involved in the D1/D1 (IgV) dimer interface over the MD simulation was calculated, showing increase in distance. Error bars represent mean ± SD. ***$p < 0.001$ by two-way ANOVA. WT, wild type.

L1, we performed a PD-L1 dimerization simulation, using a crystal structure of the PD-L1/PD-L1 dimer (PDB ID: 3FN3) as the seed model. P146R caused alterations in hydrogen bond formation in the interface between PD-L1 and PD-L1 protomer at two anti-parallel β sandwich immunoglobulin superfamily domains. Pro146 is located in domain 2 (D2), which is a typical of C1-set domains (IgC). Five hydrogen bonds were in the dimer interface (Figures 3B and 3C; Figure S3A). In the simulation, P146R caused significant alterations in these interactions except for the Ile141:Gln139 interaction, resulting in closer contacts at D2 (IgC) relative to WT PD-L1 (Figure 3D). However, P146R caused breakage of three hydrogen bonds involved in the dimer interface at domain 1 (D1) (Figures 3E and 3F; Figure S3B).

Next, we evaluated the effects of P146R on PD-1:PD-L1 interactions, using a crystal structure of the PD-1/PD-L1 complex (PDB ID: 3BIK) as the seed model (Figure 4A). Over the course of the simulation, multiple residues located at the interface between PD-1 and PD-L1 showed an increase in dynamics and loss of hydrogen bonding for P146R (Figures 4B and 4C; Figure S4), although the mutation site is located at other end of PD-L1. Taken together, these results suggest that rs17718883 weakens PD-L1 dimerization, leading to loss of PD-1:PD-L1 interactions.

PD-L1^{P146R} influences PD-L1 dimerization and the PD-1/PD-L1 complex in cells

To evaluate the functional consequences of PD-L1^{P146R} on protein-protein interactions relevant to PD-1/PD-L1 complex formation in cells, we used a cell-based fluorescence resonance energy transfer (FRET) assay. This system uses CFP (donor) and YFP (acceptor) fusions of proteins to measure protein-protein interactions (Figure 5A). In this assay, FRET is observed if donor and acceptor are in close proximity because of dimerization of their fused partners (Figure 5A). In cells where YFP is photobleached, FRET cannot occur, resulting in an increase of emission from the CFP acceptor. This increase in CFP emission after photobleaching is interpreted to mean that FRET was present prior to bleaching, and that dimers were formed (Figures S5A–S5C). The PD-1/PD-L-1 complex is a hetrotetramer consisting of a PD-1 and a PD-L1 dimer that interact with each other. We started by evaluation of the impact of P146R mutation on PD-L1 dimer formation. We co-expressed PD-L1^{WT}-CFP and PD-L1^{WT}-YFP or PD-

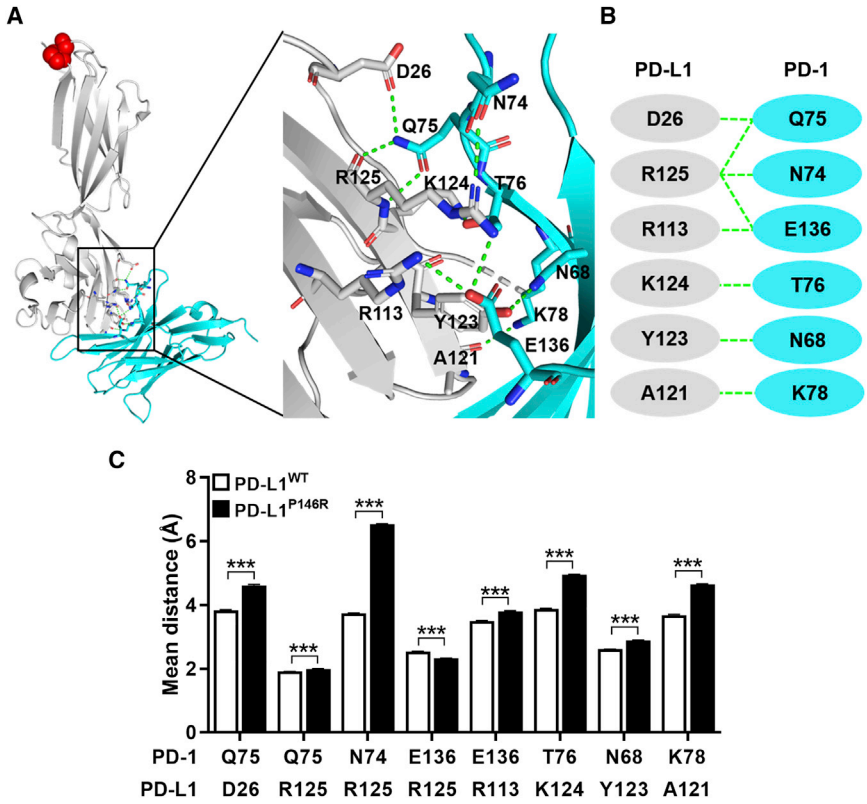

Figure 4. PD-L1^{P146R} alters PD-1:PD-L1 interactions *in silico*

(A) Molecular dynamic simulation shows interactions at the PD-1:PD-L1 interface (PDB ID: 3BIK). The residues involved in the hydrogen bonds at the dimer interfaces are shown as sticks. PD-L1 is colored in silver, and PD-1 is colored in cyan. Proline at 146 in PD-L1 is shown as a red sphere. Hydrogen bonds involved in the interface are dotted lines (green). (B) Schematic of residue contacts in 2D at the PD-1:PD-L1 dimer interface. (C) P146R widens the distance between PD-1 and PD-L1. Error bars represent mean ± SD. ***$p < 0.001$ by two-way ANOVA.

L1^{P146R}-CFP and PD-L1^{P146R}-YFP proteins in HEK293T cells and observed an increase in CFP signal after YFP bleaching in the PD-L1^{WT} setting. In contrast, there was no alteration in the CFP signal for PD-L1^{P146R}, suggesting no dimer formation (Figure 5B). Of note, WT PD-L1 displayed a phenotype consistent with membrane association, whereas PD-L1^{P146R} localization was more diffuse (Figure 5B). Together, these results establish that PD-L1^{P146R} affects PD-L1:PD-L1 interactions and cellular localization.

We next examined the interaction between PD-1 and PD-L1, using a similar experimental setup. We first examined the interaction between PD-1 and PD-1 in the absence of exogenous PD-L1. Co-expression of CFP-PD-1 and YFP-PD-1 did not show a significant increase in CFP signal following bleaching, suggesting that PD-1 does not interact with PD-1 in the absence of PD-L1 (Figure 5C). Notably, the CFP-PD-1/PD-L1^{WT}-YFP complex exhibited an increased CFP signal, consistent with the expected PD-1:PD-L1 interaction (Figure 5D). However, the introduction of P146R into PD-L1 reduced the CFP signal in the setting of CFP-PD-1 and PD-L1-YFP co-expression (Figure 5E), consistent with loss of interaction between PD-L1 and PD-1. The membrane localization of PD-1 was also influenced by PD-L1^{P146R} (Figure 5E), suggesting that PD-1:PD-1 interactions do not occur in the absence of PD-L1 and that P146R impairs PD-1/PD-L1 complex formation. This establishes that PD-L1^{P146R} impairs interactions for PD-1 and PD-L1 and PD-L1 dimerization in cells.

To further confirm that PD-L1^{P146R} alters PD-1:PD-L1 interactions, we evaluated protein stability *in situ* with a cellular thermal shift assay (CETSA).[19] Proteins that are more resistant to thermal exposure are interpreted as stabilized by other factors in CETSA, in this case, the PD-L1 protomer or PD-1. We first compared the stability between PD-L1^{WT} and PD-L1^{P146R} in the absence of PD-1. WT PD-L1 was more stable relative to PD-L1^{P146R} after thermal treatment (Figure 5F). We also compared the stability of PD-1 and PD-L1 when co-expressed in HEK293T cells. With PD-L1^{P146R}, PD-1 and PD-L1 were more susceptible to thermal treatment, with a significant loss of protein compared to WT PD-L1, suggesting that PD-L1^{P146R} disrupts the formation of PD-L1 dimers and the PD-1/PD-L1 complex and results in a decrease in protein stability upon thermal treatment.

PD-L1^{P146R} does not suppress T cell activity

Our data showed that PD-L1^{P146R} exerted reduced interaction with PD-1. This raises the possibility that cells expressing PD-L1^{P146R} will not exhibit the usual PD-L1-mediated effects on T cells. Co-culture experiments showed that inhibition of the PD-1/PD-L1 pathway using PD-L1 silencing increased cytokine interferon-γ (IFN-γ) release from T cells (Figure 6A) and T cell-induced GC cell death (Figure 6B; Figure S6) compared to control. Notably, overexpression of WT PD-L1 in PD-L1-silenced GC cells significantly inhibited cytokine IFN-γ release from T cells (Figure 6A) and T cell-induced GC cell death (Figure 6B; Figure S6). However, overexpression of PD-L1^{P146R} in PD-L1-silenced GC cells failed to inhibit IFN-γ release from T cells (Figure 6A) and T cell-induced tumor cell death compared to WT (Figure 6B; Figure S6). Animal experiments confirmed the effects of PD-L1^{P146R} on GC cell tumor formation. Immunodeficient non-obese (NOD)/severe combined immunodeficiency (SCID) mice were subcutaneously injected with SGC-7901^{KO} cells overexpressing WT or PD-L1^{P146R} after 1 week of fresh peripheral blood mononuclear cell (PBMC) injection (Figure 6C). PD-L1^{P146R} did not affect the infiltration of T cells into tumor tissues and body weight (Figures S7A–S7C). Subcutaneous

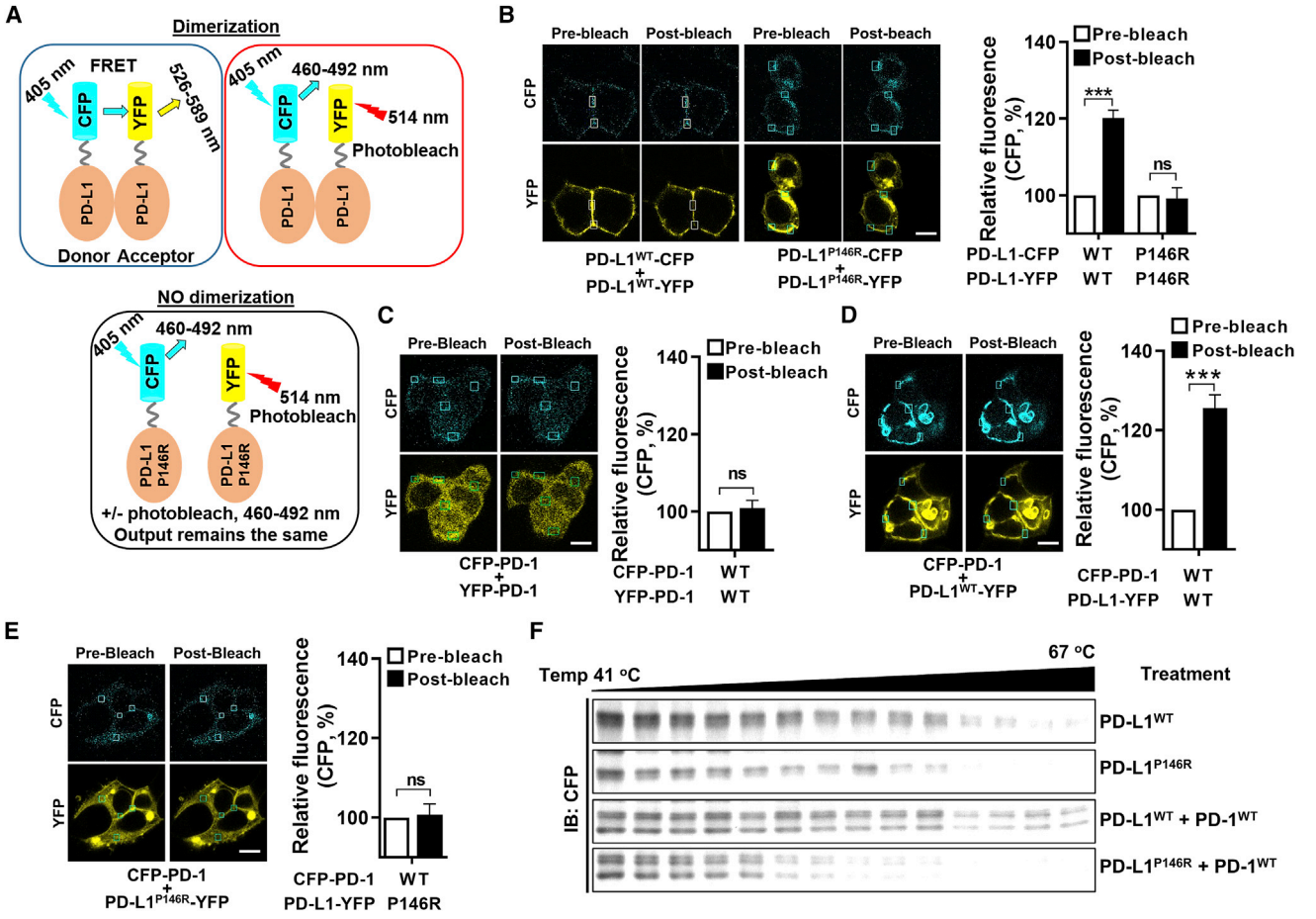

Figure 5. PD-L1^{P146R} disrupts the PD-1:PD-L1 interaction in cells

(A) Schematic diagram of the assay principle. (B) P146R impairs PD-L1:PD-L1 interactions. CFP and YFP-tagged PD-L1 wild-type (WT) or P146R were co-expressed in HEK293T cells and subjected to FRET interaction analysis. Regions of interest that were measured for FRET signal are indicated by boxes in the cell images on the left and quantification of FRET signal in the graph on the right. (C) PD-1 expressed in HEK293T cells does not dimerize. (D) PD-1 and PD-L1 interact by FRET in HEK293 cells but (E) adding the P146R substitution to PD-L1 impairs the interaction. (F) CETSA analysis shows that P146R decreases the thermal stability of both PD-1 and PD-L1 expressed in HEK293T cells. In blots with two bands, lower band is PD-1 and upper band is PD-L1. Error bars represent mean ± SEM. ***$p < 0.001$ by two-way ANOVA. Magnification, 40×, oil; scale bar, 10 μm. ns, No significance.

injection of SGC-7901 PD-L1$^{-/-}$ cells expressing WT PD-L1 formed tumors in all mice, but those expressing PD-L1^{P146R} formed tumors in only 50% of mice (Figures 6C and 6D). PBMC treatment significantly inhibited GC growth of overexpressing PD-L1^{P146R} compared to WT PD-L1 (Figure 6E). Collectively, these findings establish that PD-L1^{P146R} does not protect GC cells from activated T cell attack.

PD-1/PD-L1 blockade does not alter growth of GC expressing PD-L1^{P146R}

Loss of the PD-1:PD-L1 interaction due to PD-L1^{P146R} suggests that PD-1/PD-L1 blockade will have no therapeutic effects on GC cells expressing PD-L1^{P146R}. Co-culture experiments of cancer cells and activated T cells showed that for GC cells expressing WT PD-L1, treatment with the PD-1 antibody nivolumab significantly enhanced IFN-γ secretion from T cells (Figure 7A) and T cell-induced death (Figure 7B; Figures S8A and S8B) but did not alter cells expressing PD-L1^{P146R}. This was recapitulated *in vivo* in a NOD/SCID mouse xenograft model that utilizes SGC-7901^{KO} cells overexpressing WT PD-L1 or PD-L1^{P146R}. In these experiments, tumor-bearing mice were pre-treated with preparations of PBMCs followed by treatment with PBS or the PD-1 monoclonal antibody sintilimab (Figure 7C). Sintilimab significantly inhibited the growth of GC expressing WT PD-L1 compared to PBMC treatment alone (Figures 7D and 7E). Notably, a single treatment with PBMCs effectively suppressed the further growth of GC expressing PD-L1^{P146R}. However, our data also showed that sintilimab treatment failed to enhance the inhibitory effect of PBMCs on the growth of GC expressing PD-L1^{P146R} (Figures 7D and 7E). In addition, there was no change in body weight (Figure S8C). These findings establish that blockade of PD-1/PD-L1

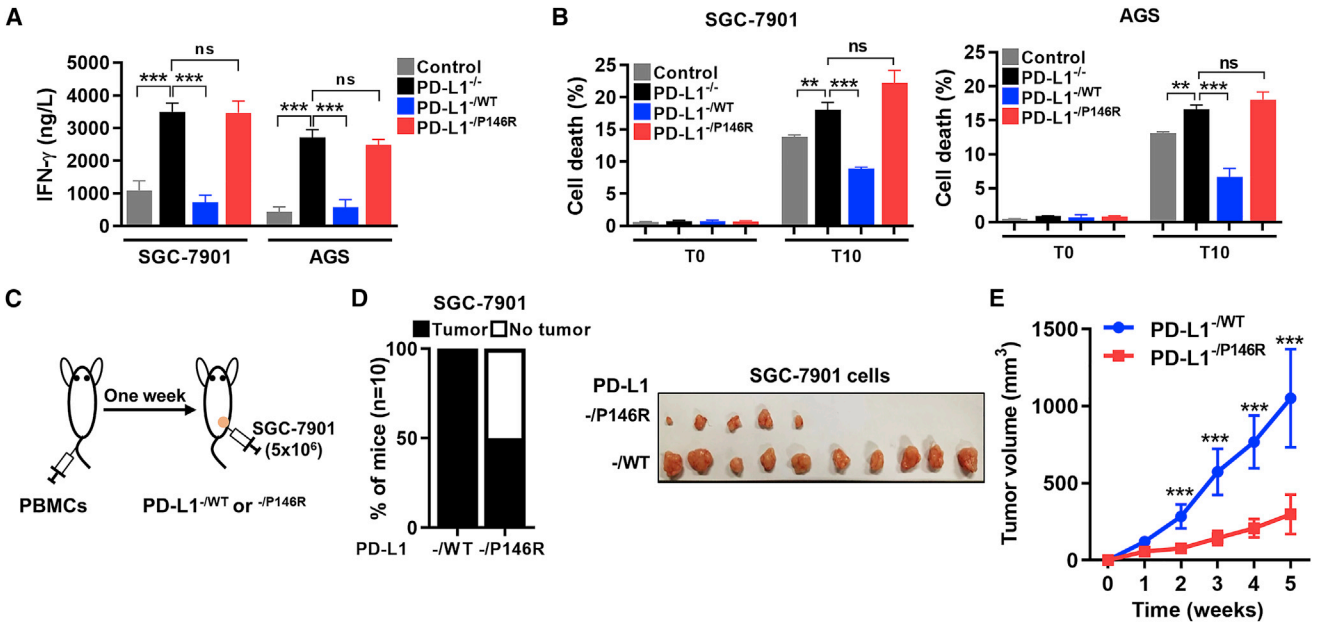

Figure 6. PD-L1^{P146R} does not alter IFN-γ secretion by T cells

(A) IFN-γ concentration does not change in the context of PD-L1$^{-/P146R}$ relative to PD-L1$^{-/-}$. GC cells and T cells were co-cultured, and the IFN-γ concentrations in cell culture supernatants were measured. (B) P146R does not change cancer cell killing ability of activated T cells relative to PD-L1$^{-/-}$. Cancer cell lysis was measured by flow cytometry after 6 h of co-culturing cancer cells and T cells. (C) Scheme for the animal experiment. (D) P146R affects tumor formation. Tumor incidence in NOD/SCID mice injected with the indicated cells and PBMCs was less in the context of PD-L1$^{-/P146R}$ relative to PD-L1$^{-/WT}$. (E) P146R attenuates tumor growth. Tumor growth curve showed dampened growth for PD-L1$^{-/P146R}$ relative to PD-L1$^{-/WT}$. Error bars represent mean ± SD. **p < 0.01; ***p < 0.001 by one-way ANOVA. WT, wild type; ns, no significance; PBMCs, peripheral blood mononuclear cells.

does not effectively inhibit GC cells expressing PD-L1^{P146R}, even in cases of high expression of PD-L1.

DISCUSSION

These data establish that PD-L1^{P146R} leads to disruption of the PD-1:PD-L1 interaction, resulting in changes in the natural history of GC and loss of efficacy for PD-1/PD-L1 blockade therapy. These results provide an important example of how genetic diversity can lead to stark differences in biological processes that impact cancer outcomes and treatment.

These data potentially apply to a sizable proportion of the world's population, given that rs17718883 has been reported in multiple different major populations including African/African-American, European, and Asian.[16,17,20,] We showed that the polymorphism is associated with a low susceptibility and better prognosis for GC. It also adds to a growing body of literature suggesting that this polymorphism has similar effects in other cancers such as hepatocellular carcinoma,[16] hematopoietic and lymphoid disorders,[21] and skin diseases.[22] In aggregate, our findings add to prior findings suggesting that rs17718883 can serve as a predictive and prognostic marker for multiple conditions.

Therapies involving PD-1/PD-L1 blockade have changed the treatment paradigms for many cancers because they are more effective and have fewer toxicities.[23,24] Nevertheless, these treatments still involve some level of risk and are costly.[5,23] Our results, showing that rs17718883 leads to resistance to PD-1/PD-L1 blockade, suggest a potential exclusion criterion that could spare a substantial segment of the population these risks and expenses.

Our study also provides a mechanistic explanation for why certain patients do not respond to PD-1/PD-L1 blockade despite expression of PD-L1. It is well established that the dimeric form of the PD-1/PD-L1 complex[25] is the physiologically active form within the context of cancer cell immune evasion. Our data support that PD-L1^{P146R} interferes with the ability of PD-L1 to form a complex with PD-1 at baseline. This is essentially equivalent to the outcome of PD-1/PD-L1 blockade therapy. Therefore, it is not surprising that this change not only influences the ability of cancer to form but also why PD-1/PD-L1 blockade therapy may not be effective in this population.

This study also provides information about the functional impact of the PD-L1^{P146R} mutation at the level of T cell activation but also raises important questions. The fact that GC still occurs within the context of rs17718883 suggests that mechanisms other than PD-1/PD-L1 may be important for immune surveillance. That this means that patients are more susceptible to elimination by activated T cells or use other pathways to evade immune surveillance are both possibilities. However, our co-culture experiments showed that GC cells with

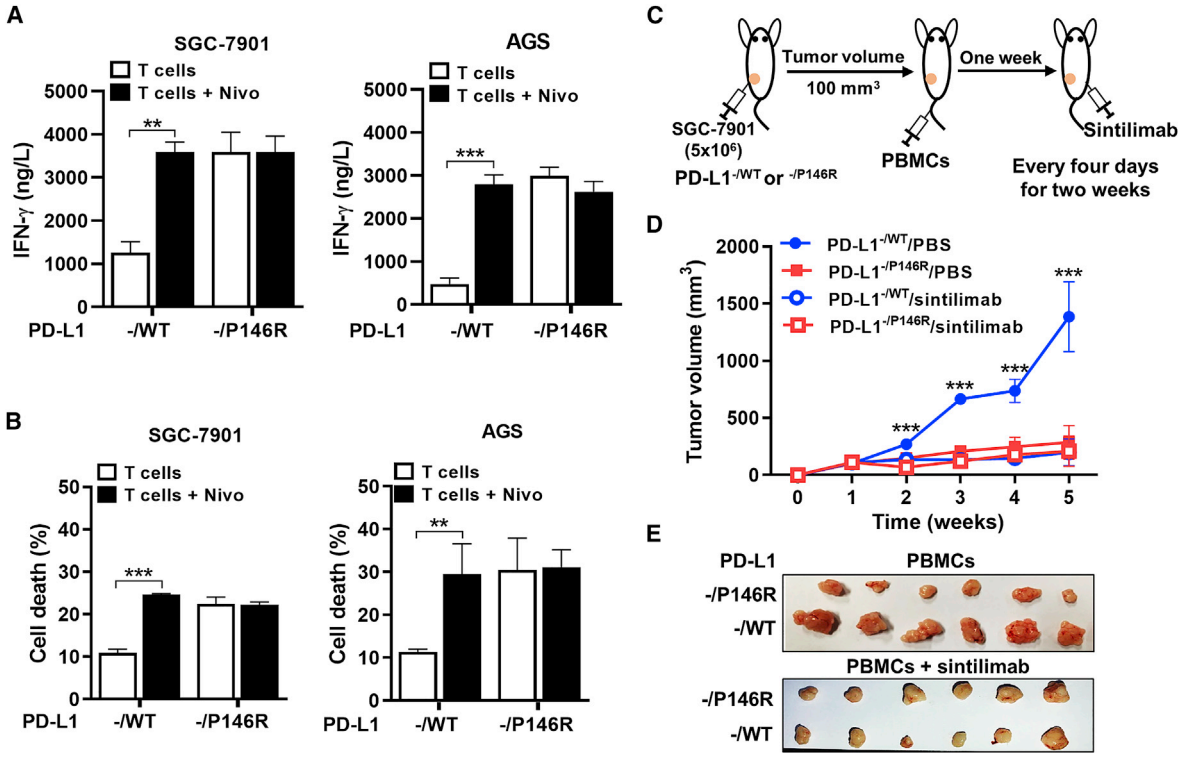

Figure 7. PD-1 monoclonal antibody treatment does not enhance T cell-mediated death of GC cells expressing PD-L1^{P146R}

(A) IFN-γ does not increase in the context of PD-L1$^{-/P146R}$ relative to PD-L1$^{-/WT}$. Co-cultures of T cells and the GC cells with or without nivolumab. IFN-γ concentration was measured in the supernatant. (B) P146R does not enhance the cancer cell killing effect in comparison to PD-L1$^{-/WT}$. Co-culture of T cells and GC cells with or without sintilimab. Cancer cell death was measured by flow cytometry. (C) A scheme for the animal experiment. (D) Sintilimab does not suppress tumor growth in the context of PD-L1$^{-/P146R}$. Tumor growth curve showed a similar suppressive effect on tumor growth in the presence or absence of sintilimab in the context of PD-L1$^{-/P146R}$. (E) Representative images of tumors are shown. Error bars represent mean ± SD. **p < 0.01; ***p < 0.001 by one-way ANOVA. WT, wild-type; nivo, nivolumab; PBMCs, peripheral blood mononuclear cells.

rs17718883 were more readily eliminated by activated T cells compared to GC cells with WT PD-L1. Because PD-1/PD-L1-mediated immune escape does not appear to happen in the setting of the rs17718883, PD-1/PD-L1 blockade does not enhance the T cell-induced tumor cell death.

In summary, our study suggests that the PD-L1 rs17718883 polymorphism is prognostic in GC and is a negative predictor of response to PD-1/PD-L1 blockade therapy in GC. This supports the use of rs17718883 as an exclusion criterion for GC patient selection in PD-1/PD-L1 blockade therapy. Nevertheless, prospective clinical studies will be required to generate high-level confirmatory evidence.

MATERIALS AND METHODS

Cell line and cell culture

HEK293T and AGS cells were obtained from American Type Culture Collection (Manassas, VA, USA), and the SGC-7901 cell line was obtained from the Chinese Academy Sciences Cell Bank of Type Culture Collection (Shanghai, China). Stable cell lines endogenous PD-L1 KO AGS and endogenous PD-L1^{KO} SGC-7901 were designated PD-L1$^{-/-}$, exhibiting the deletion of the PD-L1 gene. Stable cell lines AGS and SGC-7901 only expressing exogenous PD-L1 WT or P146R were designated as PD-L1$^{-/WT}$ or PD-L1$^{-/P146R}$. The generation of stable cell lines was performed with the CRISPR-Cas9 system as described by Burr et al.[26] HEK293T cells were cultured in DMEM (Invitrogen, Carlsbad, CA, USA) supplemented with 10% fetal bovine serum (FBS) (HyClone, Logan, UT, USA), and other cell lines were cultured in RPMI-1640 medium (Invitrogen) supplemented with 10% FBS at 37°C in humidified atmosphere containing 5% CO_2.

Human samples

Blood samples were obtained from 101 GC patients at diagnosis and 141 healthy control subjects from Daping Hospital, Chongqing, China. GC tissues were obtained from 101 patients with GC by biopsy or surgery. The characteristics of the GC patients and the control subjects are summarized in Table S1. This research was approved by the Research Ethics Board of the Daping Hospital.

DNA constructs

pcDNA3-CFP (Cat#13030), pcDNA3-YFP (Cat#13033), and pCMV-ECFP/EYFP (Cat#24520) DNA constructs were purchased from

Addgene (Watertown, MA, USA). Full-length human WT PD-L1 and PD-1 DNA oligos were obtained from IDT (Coralville, IA, USA) and amplified via PCR. CFP- or YFP-fused PD-L1 or PD-1 constructs were designed via SnapGene (GSL Biotech, Chicago, IL, USA) and generated via Gibson assembly after linearization and digestion of fragments and vectors. PD-L1^{P146R} mutant was generated via site mutagenesis using *Pfu*UItra II Hotstart PCR Master Mix (Cat#600850-51). The primers were ordered from Sigma (St. Louis, MO, USA). All PCR products were cleaned with the Select-a-Size DNA Clean & Concentrator kit from Zymo Research (Irvine, CA, USA), and the engineered DNA constructs were confirmed by DNA sequencing.

Genomic DNA amplification and polymorphism genotyping

Genomic DNA was isolated from the blood and formalin-fixed, paraffin-embedded (FFPE) tissue samples with a QIAGEN Genomic DNA Isolation Kit (Hilden, Germany) and a FastPure FFPE DNA Isolation Kit (Vazyme Biotech, Nanjing, China), respectively, according to the manufacturer's protocol. For detection of rs17718883 polymorphism, PD-L1 genes were amplified using primers of 5′-TACG TAGTTCTGTGCTCAG-3′ (forward) and 5′-GTTGATTCTCAG ;TGTGCTG-3′ (reverse). Then, these amplified products were subjected to sequencing or digested with restriction enzyme Bsr I (New England Biolabs, Ipswich, MA, USA). After restriction, the products were analyzed on 3.0% NuSiev GTG agarose gels. The WT allele (C/C) produced single bands of 259 bp; the heterozygous allele (C/G) produced three bands of 259, 163, and 96 bp; and the variant allele (G/G) produced two bands of 163 and 96 bp (Figures S1A and S1B).

Western blot and IHC

Western blot and IHC were performed as described previously.[27]

Cell viability assay

Indicated cells were transfected with the indicated plasmids. After 48 h of transfection, cells were trypsinized and reseeded in 96-well plates at a density of 5,000 cells per well, and the cell viability was measured at the indicated time with Cell Counting Kit-8 (MedChem Express, Monmouth Junction, NJ, USA), according to the manufacturer's instructions.

Immune cell isolation, activation, and cytotoxicity

PBMCs were isolated from fresh blood of healthy human donors with Lymphocyte Separation Medium according to the manufacturer's protocol (Tian Jin Hao Yang Biological Manufacture, Tianjin, China). Then, the PBMCs were incubated with human T-Activator CD3/CD28 Dynabeads and human interleukin-2 (IL-2) (30 U/mL) (Beijing T&L Biotechnology, Beijing, China) for 7 days.[28] The enrichment for $CD3^+$ T cells was identified by flow cytometry using $CD3^+$ monoclonal antibody (Invitrogen, Carlsbad, CA, USA) (Figure S9).

To investigate the effects of rs17718883 polymorphism PD-L1 on T cell-induced cytotoxicity, indicated GC cells were labeled with the LIVE/DEAD Cell-Mediated Cytotoxicity Kit (Life Technologies, Frederick, MD, USA) according to the manufacturer's protocol and co-cultivated with activated T cells at a ratio of 1:10 for 6 h. Then, GC cell lysis was monitored by flow cytometry.

To investigate the effects of PD-L1 rs17718883 polymorphism on efficacy of PD-1/PD-L1 blockade therapy in GC cells, T cells were incubated with or without 1 ng/μL PD-1 antibody nivolumab (MedChem Express) for 4 days and then co-cultivated with indicated GC cells that labeled with the LIVE/DEAD Cell-Mediated Cytotoxicity Kit (Life Technologies), at a ratio of 10:1 for 6 h. The cell lysis was measured by flow cytometry.

Molecular dynamics simulation

The Schrödinger package on the Maestro platform (Schrödinger release 2016-2, Maestro, version 10.6, Schrödinger) was used to perform molecular dynamics. Systems were prepared from high-resolution crystal structures of human PD-L1 (PDB ID: 3FN3), and PD-1/PD-L1 complex (PDB ID: 3BIK) was prepared for model construction with the Protein Preparation module, including missing atoms addition, H-bond assignment, and restrained minimization. All simulation systems were neutralized via adding charge-neutralizing counter ions in a 10-Å buffering distance in the SPC solvent model. No ion-excluded region was included. The 50-ns simulations were performed with the Desmond Molecular Dynamics module with constant temperature (300 K) and pressure (1.0 bar) in the NPT ensemble. The contacts within 4 Å were selected for analysis.

Cellular thermal shift assay

PD-1 and PD-L1 protein thermal stability was evaluated via CETSA as previously described.[19] HEK293T cells were transfected with PD-L1 WT or P146R mutant for 48 h with a supplement of 10% FBS, and then the protein samples were subjected to thermal treatment with PCR machine. In addition, the thermal stability of PD-1 and PD-L1 was performed in the setting of co-transfection of PD-L1 WT or P146R mutant with PD-1 WT-type in HEK293T cells. The resultant supernatants were then tested via western blotting assay.

FRET

First, HEK293T cells were transfected with fusion constructs containing CFP, YFP, CFP−YFP, or CFP+YFP for 36–48 h, to establish the FRET system. The CFP-YFP fusion construct functions as positive control. Live cell imaging was performed with a Confocal/Multiphoton Zeiss LSM880 microscope. CFP was excited with 405-nm light, and emission was monitored over the range of 460–492 nm; YFP was excited with 514-nm light, and emission was monitored over the range of 526–589 nm. YFP was photobleached with the 514-nm laser line at 80% power for 1 min. An image of CFP fluorescence and YFP fluorescence after photobleaching was obtained with the respective filter sets. Data were collected from 10–12 different cells in different fields from the same coverslip. Two to three regions of interest (located on the cell membrane) in the photobleached area were selected per cell, and the mean CFP fluorescence before and after photobleaching was obtained with ZEN software.

To examine PD-L1 dimerization, HEK293T cells were co-transfected with PD-L1^{WT}-CFP and PD-L1^{WT}-YFP or PD-L1^{P146R}-CFP and PD-L1^{P146R}-YFP plasmids, respectively. In addition, HEK293T cells were co-transfected with CFP-PD-1 WT and PD-L1^{WT}-YFP or CFP-PD-1 WT and PD-L1^{P146R}-YFP plasmids, respectively. Cells were subjected to microscopy 36–48 h after transfection.

Animal experiments

To investigate the effects of PD-L1 rs17718883 polymorphisms (PD-L1^{P146R}) on gastric tumor growth, 1×10^7 indicated GC cells in 100 μL of PBS were subcutaneously injected into 6-week-old female nude mice (5 mice per group) and the tumor volumes were measured once a week.

To investigate PD-L1^{P146R} effects on T cell-induced inhibition of gastric tumor formation, 3×10^6 fresh PBMCs isolated from a healthy human donor were injected into the lateral tail vein of 6-week-old female NOD/SCID mice (10 mice per group). After 1 week of PBMC injection, 1×10^7 SGC-7901^{KO} cells that overexpress WT PD-L1 or PD-L1^{P146R} in 100 μL of PBS were subcutaneously injected into mice and the tumor volumes were measured once a week.

To investigate PD-L1^{P146R} effects on efficacy of PD-1/PD-L1 blockade therapy in GC, 1×10^7 SGC-7901^{KO} cells that overexpress WT PD-L1 or PD-L1^{P146R} in 100 μL of PBS were subcutaneously injected into 6-week-old female NOD/SCID mice. When the mean tumor size reached ~100 mm^3, 3×10^6 PBMCs were injected into mice through the lateral tail vein. After 1 week of PBMC injection, mice were treated with PBS or PD-1 antibody sintilimab (Innovent Biologics, Jiangsu, China) by intraperitoneal (i.p.) injection (1 mg/kg body weight) every 4 days for 2 weeks (6 mice per group). These animal studies were approved by the Research Ethics Board of the Daping Hospital.

Statistical analysis

The Hardy-Weinberg equilibrium analysis for genotype distribution in controls and cases was carried out according to the literature. Statistical analyses were performed with SPSS (IBM SPSS Statistics 19, SPSS, Chicago, IL, USA). A statistical analysis to compare distributions was performed with the χ^2 test. Odds ratios (ORs) and 95% confidence intervals (CIs) were calculated with binary logistic regression. Survival curves for OS were determined with the Kaplan-Meier method, and the log rank test was used to generate p values. Multivariate Cox proportional hazards models (forward stepwise: likelihood ratio) were used to estimate adjusted hazard ratios (HRs) with 95% CIs. Multivariable regression analysis was adjusted for age, gender, ECOG stage, histology, disease stage, smoking status, and treatment methods. FRET data are expressed as mean ± SEM, and the rest are presented as mean ± SD. Two-sided p values < 0.05 were considered statistically significant.

SUPPLEMENTAL INFORMATION

Supplemental information can be found online at https://doi.org/10.1016/j.ymthe.2021.09.013.

ACKNOWLEDGMENTS

This work was supported by the Science and Technology Innovation Enhancement Project of Army Medical University (STIEP, 2019XLC3052, to Q.L.) and the National Natural Science Foundation of China (81772495, to D.W.). This work was also supported by NIH P30CA142543 (to K.D.W.).

AUTHOR CONTRIBUTIONS

Study concept and design: Q.L., Z.-W.Z., D.W., K.D.W., and C.-X.X.; acquisition of data: Q.L., Z.-W.Z., J.L., S.-N.W., Y.P., M.-S.D., H.L., and G.-B.S.; analysis and interpretation of data: Q.L., Z.-W.Z., J.L., S.-N.W., Y.P., M.-S.D., H.L., and G.-B.S.; drafting of the manuscript: Z.-W.Z., K.D.W., and C.-X.X.; statistical analysis: Q.L., Z.-W.Z., and J.L.; technical or material support: J.-M.W., X.W., and S.-N.W.; study supervision: D.W., K.D.W., and C.-X.X..

DECLARATION OF INTERESTS

K.D.W. has received consulting fees from Sanofi Oncology, is a member of the SAB for Vibliome Therapeutics, and has or had sponsored research agreements with Astellas Pharmaceuticals and Revolution Medicine. K.D.W. declares that none of these relationships is directly or indirectly related to the content of this manuscript. The other authors declare no competing interests.

REFERENCES

1. Ferlay, J., Colombet, M., Soerjomataram, I., Mathers, C., Parkin, D.M., Piñeros, M., Znaor, A., and Bray, F. (2019). Estimating the global cancer incidence and mortality in 2018: GLOBOCAN sources and methods. Int. J. Cancer *144*, 1941–1953.
2. den Hoed, C.M., and Kuipers, E.J. (2016). Gastric Cancer: How Can We Reduce the Incidence of this Disease? Curr. Gastroenterol. Rep. *18*, 34.
3. Song, Z., Wu, Y., Yang, J., Yang, D., and Fang, X. (2017). Progress in the treatment of advanced gastric cancer. Tumour Biol. *39*, 1010428317714626.
4. Wang, B.C., Zhang, Z.J., Fu, C., and Wang, C. (2019). Efficacy and safety of anti-PD-1/PD-L1 agents vs chemotherapy in patients with gastric or gastroesophageal junction cancer: a systematic review and meta-analysis. Medicine (Baltimore) *98*, e18054.
5. Fuchs, C.S., Doi, T., Jang, R.W., Muro, K., Satoh, T., Machado, M., Sun, W., Jalal, S.I., Shah, M.A., Metges, J.P., et al. (2018). Safety and Efficacy of Pembrolizumab Monotherapy in Patients With Previously Treated Advanced Gastric and Gastroesophageal Junction Cancer: Phase 2 Clinical KEYNOTE-059 Trial. JAMA Oncol. *4*, e180013.
6. Yi, M., Jiao, D., Xu, H., Liu, Q., Zhao, W., Han, X., and Wu, K. (2018). Biomarkers for predicting efficacy of PD-1/PD-L1 inhibitors. Mol. Cancer *17*, 129.
7. Tumeh, P.C., Harview, C.L., Yearley, J.H., Shintaku, I.P., Taylor, E.J.M., Robert, L., Chmielowski, B., Spasic, M., Henry, G., Ciobanu, V., et al. (2014). PD-1 blockade induces responses by inhibiting adaptive immune resistance. Nature *515*, 568–571.
8. Jiang, X., Wang, J., Deng, X., Xiong, F., Ge, J., Xiang, B., Wu, X., Ma, J., Zhou, M., Li, X., et al. (2019). Role of the tumor microenvironment in PD-L1/PD-1-mediated tumor immune escape. Mol. Cancer *18*, 10.
9. Dong, H., Strome, S.E., Salomao, D.R., Tamura, H., Hirano, F., Flies, D.B., Roche, P.C., Lu, J., Zhu, G., Tamada, K., et al. (2002). Tumor-associated B7-H1 promotes T-cell apoptosis: a potential mechanism of immune evasion. Nat. Med. *8*, 793–800.
10. Wu, C., Zhu, Y., Jiang, J., Zhao, J., Zhang, X.G., and Xu, N. (2006). Immunohistochemical localization of programmed death-1 ligand-1 (PD-L1) in gastric carcinoma and its clinical significance. Acta Histochem. *108*, 19–24.
11. Kim, S.T., Cristescu, R., Bass, A.J., Kim, K.M., Odegaard, J.I., Kim, K., Liu, X.Q., Sher, X., Jung, H., Lee, M., et al. (2018). Comprehensive molecular characterization of clinical responses to PD-1 inhibition in metastatic gastric cancer. Nat. Med. *24*, 1449–1458.

12. Wang, Z., and Moult, J. (2001). SNPs, protein structure, and disease. Hum. Mutat. *17*, 263–270.

13. Zou, J., Wu, D., Li, T., Wang, X., Liu, Y., and Tan, S. (2019). Association of PD-L1 gene rs4143815 C>G polymorphism and human cancer susceptibility: A systematic review and meta-analysis. Pathol. Res. Pract. *215*, 229–234.

14. Lee, S.Y., Jung, D.K., Choi, J.E., Jin, C.C., Hong, M.J., Do, S.K., Kang, H.G., Lee, W.K., Seok, Y., Lee, E.B., et al. (2016). PD-L1 polymorphism can predict clinical outcomes of non-small cell lung cancer patients treated with first-line paclitaxel-cisplatin chemotherapy. Sci. Rep. *6*, 25952.

15. Nomizo, T., Ozasa, H., Tsuji, T., Funazo, T., Yasuda, Y., Yoshida, H., Yagi, Y., Sakamori, Y., Nagai, H., Hirai, T., and Kim, Y.H. (2017). Clinical Impact of Single Nucleotide Polymorphism in PD-L1 on Response to Nivolumab for Advanced Non-Small-Cell Lung Cancer Patients. Sci. Rep. *7*, 45124.

16. Xie, Q., Chen, Z., Xia, L., Zhao, Q., Yu, H., and Yang, Z. (2018). Correlations of PD-L1 gene polymorphisms with susceptibility and prognosis in hepatocellular carcinoma in a Chinese Han population. Gene *674*, 188–194.

17. Wang, S.C., Lin, C.H., Li, R.N., Ou, T.T., Wu, C.C., Tsai, W.C., Liu, H.W., and Yen, J.H. (2007). Polymorphisms of genes for programmed cell death 1 ligands in patients with rheumatoid arthritis. J. Clin. Immunol. *27*, 563–567.

18. Lee, S.Y., Jung, D.K., Choi, J.E., Jin, C.C., Hong, M.J., Do, S.K., Kang, H.G., Lee, W.K., Seok, Y., Lee, E.B., et al. (2017). Functional polymorphisms in PD-L1 gene are associated with the prognosis of patients with early stage non-small cell lung cancer. Gene *599*, 28–35.

19. Jafari, R., Almqvist, H., Axelsson, H., Ignatushchenko, M., Lundbäck, T., Nordlund, P., and Martinez Molina, D. (2014). The cellular thermal shift assay for evaluating drug target interactions in cells. Nat. Protoc. *9*, 2100–2122.

20. Karczewski, K.J., Francioli, L.C., Tiao, G., Cummings, B.B., Alföldi, J., Wang, Q., Collins, R.L., Laricchia, K.M., Ganna, A., Birnbaum, D.P., et al.; Genome Aggregation Database Consortium (2020). The mutational constraint spectrum quantified from variation in 141,456 humans. Nature *581*, 434–443.

21. Tessoulin, B., Moreau-Aubry, A., Descamps, G., Gomez-Bougie, P., Maïga, S., Gaignard, A., Chiron, D., Ménoret, E., Le Gouill, S., Moreau, P., et al. (2018). Whole-exon sequencing of human myeloma cell lines shows mutations related to myeloma patients at relapse with major hits in the DNA regulation and repair pathways. J. Hematol. Oncol. *11*, 137.

22. Zehir, A., Benayed, R., Shah, R.H., Syed, A., Middha, S., Kim, H.R., Srinivasan, P., Gao, J., Chakravarty, D., Devlin, S.M., et al. (2017). Mutational landscape of metastatic cancer revealed from prospective clinical sequencing of 10,000 patients. Nat. Med. *23*, 703–713.

23. Topalian, S.L., Hodi, F.S., Brahmer, J.R., Gettinger, S.N., Smith, D.C., McDermott, D.F., Powderly, J.D., Carvajal, R.D., Sosman, J.A., Atkins, M.B., et al. (2012). Safety, activity, and immune correlates of anti-PD-1 antibody in cancer. N. Engl. J. Med. *366*, 2443–2454.

24. Chen, L., and Han, X. (2015). Anti-PD-1/PD-L1 therapy of human cancer: past, present, and future. J. Clin. Invest. *125*, 3384–3391.

25. Lin, D.Y., Tanaka, Y., Iwasaki, M., Gittis, A.G., Su, H.P., Mikami, B., Okazaki, T., Honjo, T., Minato, N., and Garboczi, D.N. (2008). The PD-1/PD-L1 complex resembles the antigen-binding Fv domains of antibodies and T cell receptors. Proc. Natl. Acad. Sci. USA *105*, 3011–3016.

26. Burr, M.L., Sparbier, C.E., Chan, Y.C., Williamson, J.C., Woods, K., Beavis, P.A., Lam, E.Y.N., Henderson, M.A., Bell, C.C., Stolzenburg, S., et al. (2017). CMTM6 maintains the expression of PD-L1 and regulates anti-tumour immunity. Nature *549*, 101–105.

27. Xu, C.X., Jere, D., Jin, H., Chang, S.H., Chung, Y.S., Shin, J.Y., Kim, J.E., Park, S.J., Lee, Y.H., Chae, C.H., et al. (2008). Poly(ester amine)-mediated, aerosol-delivered Akt1 small interfering RNA suppresses lung tumorigenesis. Am. J. Respir. Crit. Care Med. *178*, 60–73.

28. Vizcardo, R., Masuda, K., Yamada, D., Ikawa, T., Shimizu, K., Fujii, S., Koseki, H., and Kawamoto, H. (2013). Regeneration of human tumor antigen-specific T cells from iPSCs derived from mature CD8(+) T cells. Cell Stem Cell *12*, 31–36.